Interaction of vortices in superconductors with κ close to $1/\sqrt{2}$

F. Mohamed*, M. Troyer, and G. Blatter
Theoretische Physik, ETH-Hönggerberg, CH-8093 Zürich, Switzerland

I. Luk'yanchuk
L. D. Landau Institute for Theoretical Physics, Moscow, Russia
and Institut Laue Langevin, BP156 38042 Grenoble Cedex 9, France

Using a perturbative approach to the infinitely degenerate Bogomolnyi vortex state for a superconductor with $\kappa=1/\sqrt{2}, T \to T_c$, we calculate the interaction of vortices in a superconductor with κ close to $1/\sqrt{2}$. We find, numerically and analytically, that depending on the material the interaction potential between the vortices varies with decreasing κ from purely repulsive (as in a type-II superconductor) to purely attractive (as in a type-I superconductor) in two different ways: either vortices form a bound state and the distance between them changes gradually from infinity to zero or this transition occurs in a discontinuous way as a result of a competition between minima at infinity and zero. We study the discontinuous transition between the vortex and Meissner states caused by the nonmonotonous vortex interaction and calculate the corresponding magnetization jump.

I. INTRODUCTION

It is widely known that superconducting vortices repel each other in superconductors of type II and attract each other in superconductors of type I. The physical origin of this phenomenon is the competition between the magnetic repulsion of the vortices (dominating in type-II superconductors) and the gain in condensation energy of overlapping vortex cores producing an attractive interaction (dominating in type-I superconductors). Within the Ginzburg-Landau (GL) approximation it can easily be seen that the long-range asymptotic behavior of the vortex interaction changes its sign at $\kappa=1/\sqrt{2}$. The vortex interaction is[1]

$$U_{\text{int}}(l)=2\pi c^2(\kappa)K_0(l)-\frac{\pi}{\kappa^2}d(\kappa)^2 K_0(\sqrt{2}\kappa l),\quad (1)$$

where $K_0(l)$ is the modified Bessel function of zero order, and $c(\kappa)$ and $d(\kappa)$ are slowly varying functions of κ that are equal at $\kappa=1/\sqrt{2}$. The detailed profile of $U_{\text{int}}(l)$ at any l when κ goes through $1/\sqrt{2}$ was, however, calculated only in the 1970s by Jacobs and Rebbi[2] using a special symmetry of the z-invariant GL equations at $\kappa=1/\sqrt{2}$ discovered by Bogomolnyi.[3] According to Bogomolnyi, Jacobs, and Rebbi (BJR) the GL energy at $\kappa=1/\sqrt{2}$ is degenerate with respect to any configuration of vortices. The sign change of $U_{\text{int}}(l)$ at $\kappa=1/\sqrt{2}$ is an *exact* result of the GL theory: at $\kappa>1/\sqrt{2}$ the interaction is purely repulsive, at $\kappa=1/\sqrt{2}$ vortices do not interact, and at $\kappa<1/\sqrt{2}$ the interaction is purely attractive.

Experiments,[4,5] however, reveal a more complex situation. The interaction potential $U_{\text{int}}(l)$ close to $\kappa=1/\sqrt{2}$ was sometimes found to be attractive at large distances and repulsive at short ones. This nonmonotonous profile of $U_{\text{int}}(l)$ manifests itself as a discontinuous transition between vortex and Meissner states and by the existence of intermediate mixed-state domains of bound vortices. The presence of a local minimum in $U_{\text{int}}(l)$ at $\kappa \sim 1/\sqrt{2}$ can be explained (as we do here) by taking into account low-temperature corrections to the GL theory that modify the almost flat profile of the interaction.[6] Another possibility is to take into account the coupling of the order parameter gradient with the crystalline strain, $u_{ij}\partial_i\Psi\partial_j\Psi^*$, or to consider the fluctuations and anisotropies in the vortex lattice, which produce an attractive interaction of the van der Waals type.[7]

Several calculations based on an extended GL functional[8] were done to clarify this issue. Jacobs[6] calculated low-temperature corrections to the long-range vortex interaction (1) and found that vortices attract each other already in type-II superconductors. Based on his results Hubert[9] performed numerical calculations for a periodic Abrikosov lattice of vortices and demonstrated the nonmonotonous behavior of the vortex interaction in a vortex lattice. These calculations are consistent with numerical variational calculations by Brandt[10] based on Gorkov equations and solved for vortex lattice configurations at all possible values of H, T, and κ. Although these results reproduce a nontrivial behavior of $U_{\text{int}}(l)$ at $\kappa \sim 1/\sqrt{2}$, it is difficult to survey and interpret them in a systematic way because of the cumbersome mathematics and large number of terms in the extended GL functional.

A new method of calculating the properties of superconductors near $\kappa \sim 1/\sqrt{2}$ has been developed recently.[11] In this approach the degenerate vortex state at $\kappa=1/\sqrt{2}$ and with the external field H equal to the thermodynamic critical field H_c is considered as the starting point of a secular perturbation theory. A degeneracy-lifting perturbation functional in the small parameters

$$\gamma=\kappa^2-\frac{1}{2},\quad t=\frac{T}{T_c}-1 \qquad (2)$$

is constructed. This approach avoids bulky calculations and allows us to describe the superconductor with $|\gamma|, |t| \ll 1$ in a form that is easy to interpret.

We will use this perturbation approach to calculate the interaction $U_{\text{int}}(l)$ between two separate vortices and between vortices in a lattice for a superconductor with $\kappa \sim 1/\sqrt{2}$ when the Ginzburg-Landau theory is extended to low temperatures. We consider the isotropic superconductors. The case when the crystal anisotropy that manifests itself in the second- and fourth-order gradient terms of the Ginzburg-Landau functional is important requires special consideration. We study the discontinuous transition between the vortex and Meissner states caused by the nonmonotonous vortex interaction and calculate the corresponding magnetization jump.

II. PERTURBATION APPROACH

We start by outlining the main elements of our perturbative approach.[11] According to Bogomolnyi[3] and Jacobs and Rebbi,[2] in a z-invariant situation, with $H = H_c$, the order parameter amplitude $|\psi(\mathbf{r}, \mathbf{r}_1, \ldots, \mathbf{r}_n)|$ of vortices located at $\mathbf{r} = \mathbf{r}_1, \ldots, \mathbf{r}_n$ in a superconductor with $\gamma = 0$, $t \to 0$ is described by the BJR equation

$$\frac{1}{2}\nabla^2 \ln|\psi|^2 = |\psi|^2 - 1 + \sum_i 2\pi\delta(\mathbf{r} - \mathbf{r}_i). \quad (3)$$

The magnetic field inside the sample is uniquely related to $|\psi(\mathbf{r})|$ via

$$b(\mathbf{r}) = 1 - |\psi(\mathbf{r})|^2. \quad (4)$$

Here, dimensionless variables $\psi = \Psi/\Psi_0, b = \sqrt{2}\kappa B/H_c$ are used (with Ψ_0 the uniform order parameter when the external field $H = 0$). Distances are measured in units of the coherence length ξ.

Since at $\gamma = 0, t \to 0$ the vortices do not interact, the vortex energy close to this point can be calculated to first order in γ and t by substituting the unperturbed solution $|\psi(\mathbf{r}, \mathbf{r}_1, \ldots, \mathbf{r}_n)|$ of Eq. (3) into the functional

$$f = (h_0 - h_{c2})|\psi|^2 + (\gamma - c_4 t)|\psi|^4 - c_6 t|\psi|^6 \quad (5)$$

as obtained in Ref. 11 and defined for the class of Bogomolnyi solutions. Here $f = 8\pi\kappa^2\mathcal{F}/H_c^2 + \kappa^2$ ($\mathcal{F}$ is the GL free energy) and $h_{c2} = \sqrt{2}\kappa H_{c2}/H_c$ are the dimensionless free energy and the upper critical field. The functional (5) accounts for all the terms of the extended GL functional that are assembled into the terms $|\psi|^4$ and $|\psi|^6$ with experimentally measurable material coefficients c_4 and c_6. The parameter c_4 is always positive, whereas c_6 can be both positive and negative.

To calculate the energy of vortices located at $\mathbf{r} = \mathbf{r}_1, \ldots, \mathbf{r}_n$ one should solve first the BJR equation (3) and then substitute this solution into the perturbation functional (5). The analytical aspects of this task have been discussed in detail in Ref. 11; here we solve the BJR equation (3) numerically by a finite-elements method on an adaptive grid by using the ansatz

$$|\psi(\mathbf{r})| = \prod_k |\mathbf{r} - \mathbf{r}_k| e^{\varphi(\mathbf{r})/2}. \quad (6)$$

Using this ansatz, the BJR equations are reduced to a nonlinear Poisson-like equation for φ and the δ functions are removed. In a weak formulation for the finite-dimensional space $[\varphi(\mathbf{r}) = \Sigma_i \varphi_i p_i(\mathbf{r})]$, the problem is written as

$$-\frac{1}{2}\sum_j \varphi_j \int_\Omega \nabla p_j \cdot \nabla p_i d\mathbf{r}$$

$$= -\frac{1}{2}\int_{\partial\Omega} p_i \nabla\varphi \times d\mathbf{l} + \int_\Omega \left[\exp\left(\sum_j p_j\varphi_j \right) \right.$$

$$\left. \times \prod_k |\mathbf{r} - \mathbf{r}_k|^2 - 1 \right] p_i d\mathbf{r}, \quad (7)$$

where $p_j(\mathbf{r})$ are Lagrange elements on a quadratic grid.[12] We linearize the exponential function and iterate the resulting linear part. The dynamic refinement is based on the normal Kelly indicator[13] for the local error and on the error evaluation of the nonlinear exponential part.

As boundary conditions we use either Neumann (specifying $\partial_\perp |\psi|$) or periodic boundary conditions. In the Neuman case the normal derivative of φ is taken to be $\partial_\perp \varphi = -2\Sigma_k \partial_\perp \ln(|\mathbf{r} - \mathbf{r}_k|)$. In the periodic case a special constraint is added to the system of linear equations for $\varphi_i \in \mathbb{R}$, to compensate for the nonperiodicity of $\Sigma_k \ln(|\mathbf{r} - \mathbf{r}_k|)$. This algorithm is implemented in C++ using the deal-II library[12,14] for the finite-elements calculations.

III. TWO VORTEX INTERACTION

We now use the above method to calculate the interaction energy $U_{\text{int}}(l)$ between two vortices located at $\mathbf{r}_{1,2} = \pm \mathbf{l}/2$ by subtracting the self-energy of separated vortices $2\varepsilon_1$ from the two-vortex energy $\varepsilon_{1,1}(l)$,

$$U_{\text{int}}(l) = \varepsilon_{1,1}(l) - 2\varepsilon_1 = \varepsilon_{1,1}(l) - \varepsilon_{1,1}(\infty). \quad (8)$$

As follows from Eq. (5) the energy $U_{\text{int}}(l)$ can be written as a superposition of two structure functions $u_k(l)$, $k = 4,6$,

$$U_{\text{int}}(l) = (\gamma - c_4 t)u_4(l) - c_6 t u_6(l), \quad (9)$$

which do not depend on the material parameters γ, c_4, and c_6,

$$u_k(l) = \int \{[1 - |\psi(\mathbf{r}, \mathbf{r}_1, \mathbf{r}_2)|^k] - [1 - |\psi(\mathbf{r}, \mathbf{r}_1)|^k]$$

$$- [1 - |\psi(\mathbf{r}, \mathbf{r}_2)|^k]\} dS. \quad (10)$$

Here $\psi(\mathbf{r}, \mathbf{r}_{1,2})$ and $\psi(\mathbf{r}, \mathbf{r}_1, \mathbf{r}_2)$ are the one- and two-vortex solutions of Eq. (3). Note that[11] $u_2(l) = 0$.

It follows from Eq. (9) that the profile of $U_{\text{int}}(l)$ depends only on the sign of c_6 and on the control parameter

$$d = \frac{\gamma - c_4 t}{|c_6 t|}. \quad (11)$$
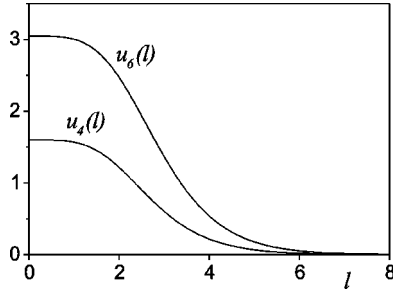
FIG. 1. Structure functions $u_4(l)$ and $u_6(l)$ for two vortices separated by a distance l. Appropriate superposition of $u_4(l)$ and $u_6(l)$ gives the vortex interaction energy $U_{\text{int}}(l)$. The distance l is measured in units of the coherence length ξ.

In Fig. 1 we show the result of our numerical calculations of $u_4(l)$ and $u_6(l)$.

With the numerical method outlined in Sec. II we can calculate the minimum of U_{int} for $1.4 \leq d \leq 2.7$. For $d < 1.4$ and for $d > 2.7$ the minimum cannot be reliably found because of the flat profile of $U_{\text{int}}(l)$ at small and large values of l. To determine the behavior of $U_{\text{int}}(l)$ at $l \ll 1$ and at $l \gg 1$ we have used the analytic estimates of Ref. 11 that are summarized below.

(i) The order parameter of the widely separated weakly overlapping vortices ($l \gg 1$) can be approximated as

$$|\psi(\mathbf{r})|^2 = g_1^2(\mathbf{r} + \mathbf{l}/2) + g_1^2(\mathbf{r} - \mathbf{l}/2) - 1, \quad (12)$$

where $g_1(\mathbf{r})$ is the axially symmetric one-quantum vortex solution of the BJR equation. The long-range interaction is written as [up to the slow preexponential factor $u(l)$]

$$U_{\text{int}}(l) = [\gamma - (c_4 + 3c_6)t] u(l) e^{-4l}, \quad (13)$$

and becomes attractive when γ is smaller than the critical value

$$\gamma_{c1} = (c_4 + d_{c1} c_6)t, \quad d_{c1} = 3. \quad (14)$$

Equation (13) has been obtained before in Ref. 6 and generalizes Eq. (1) to lower temperatures.

(ii) The order parameter of two close-lying vortices with almost coinciding cores ($l \ll 1$) can be approximated as

$$|\psi(\mathbf{r})| = g_2(r) + \frac{1}{8} g_2(r)(\mathbf{l}\nabla)^2 \ln g_2(r), \quad (15)$$

where $g_2(\mathbf{r})$ is the axially symmetric two-quantum vortex solution of the BJR equation. At small l the short-range vortex interaction is expanded as

$$U_{\text{int}}(l) = [0.91(\gamma - c_4 t) - 1.13 c_6 t] l^2 + O(l^4). \quad (16)$$

It is attractive when the second-order term is negative, i.e., when γ is smaller than the critical value

$$\gamma_{c2} = (c_4 + d_{c2} c_6)t, \quad d_{c2} = 1.26. \quad (17)$$

We finally compare the energy of a two-quantum vortex to the energy of two widely separated one-quantum vortices.
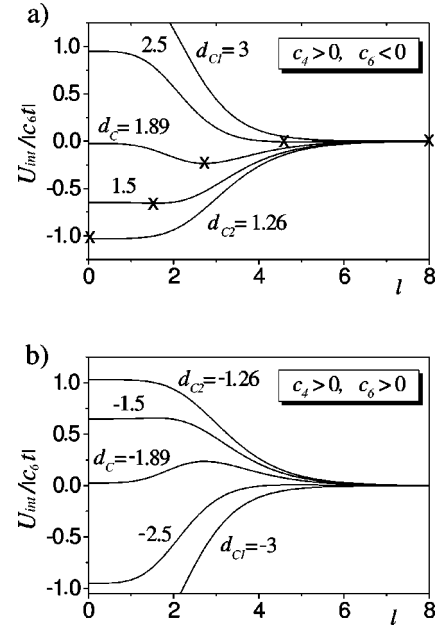
FIG. 2. The reduced two-vortex interaction energy $U_{\text{int}}(l)/|c_6 t|$ at different parameters $d = (\gamma - c_4 t)/|c_6 t|$ (a) for $c_4 > 0, c_6 < 0$ (crosses indicate the minima) and (b) for $c_4 > 0, c_6 > 0$.

A two-quantum vortex becomes energetically more favorable when γ is smaller than the critical value

$$\gamma_c = (c_4 + d_c c_6)t, \quad d_c = 1.89. \quad (18)$$

This value always lies in between γ_{c1} and γ_{c2}. The critical parameter d_{c1} remains unchanged in the case of interacting multiquantum vortices whereas the numerical coefficients d_{c2} in Eq. (17) and d_c in Eq. (18) become larger.

Combining these numerical and analytical results we conclude that depending on the parameters c_6 and c_4 two scenaria are possible for the evolution of $U_{\text{int}}(l)$ as function of d.

(I) The case $c_4 > 0, c_6 < 0$ is shown in Fig. 2(a). When $d > d_{c1} = 3$ the interaction is purely repulsive. Below d_{c1} we find an attraction at large distances while the short-range interaction remains repulsive. The vortices form a bound state with an equilibrium distance $l_0(d)$ corresponding to the minimum of $U_{\text{int}}(l)$. Finally, below the second critical value $d_{c2} = 1.26$, the short-range interaction becomes attractive too and the vortices combine into a two-quantum vortex.

The distance $l_0(d)$ of two bound vortices, shown in Fig. 3, diverges as $-\ln(d_{c1} - d)$ for $d \to d_{c1}$ and vanishes as $\sqrt{d - d_{c2}}$ for $d \to d_{c2}$. Special care has to be taken to observe these vortex bound states. One can try, e.g., to obtain pinned vortex molecules after expelling other vortices from the sample by turning off the external field.

(II) The case $c_6 > 0, c_4 > 0$ is shown in Fig. 2(b). The order of the critical parameters d_{c2} and d_{c1} is now reversed, $d_{c1} < d_{c2}$. The vortex interaction now changes its sign at negative d. When $d > d_{c2} = -1.26$ the interaction is purely repulsive. Below d_{c2} the interaction becomes short-range attractive while retaining its long-range repulsive character. Below $d_{c1} = -3$ the interaction is purely attractive. The
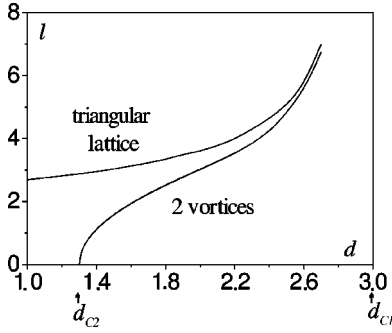
FIG. 3. Distance between two bound vortices as a function of the material parameter d (when $c_4 > 0, c_6 < 0$). The equilibrium vortex distance in the regular triangular vortex lattice at discontinuous transition at $H = H_{c1}^*$ is shown for comparison.

FIG. 4. Structure functions $v_4(l)$ and $v_6(l)$ for the square (90°), triangular (60°), and rhombic (45°) lattices with lattice constant l. Superposition of $v_4(l)$ and $v_6(l)$ gives the lattice interaction function $(z/2)U_{\text{lat}}(l)$. The distance is measured in units of the coherence length ξ.

equilibrium vortex configuration in the interval $d_{c1} < d < d_{c2}$ is thus determined by the competition between two local minima of $U_{\text{int}}(l)$ at $l = 0$ and at $l = \infty$. The formation of a two-quantum vortex becomes more favorable than two isolated and widely separated vortices below the critical value $d_c = -1.89$. The parameters d_{c1} and d_{c2} then serve as supercooling and superheating limits of d.

The cases considered above exhaust all possible scenarios for the evolution of $U_{\text{int}}(l)$ near the Bogomolnyi point. Case (I) seems to be more realistic given the typical values of the material constants[11]: $c_4 \sim 0.1$–0.5 and $c_6 \sim -0.2$–0.

We conclude this section by remarking that the vortex-antivortex interaction cannot be calculated in this formalism since the vortex-antivortex pair does not belong to the degenerate set of the Bogomolnyi states at $\kappa = 1/\sqrt{2}$. Moreover, unlike the case of parallel vortices, both the magnetic and the condensation energy contribute equally to the attractive vortex-antivortex interaction and thus there is no critical point at $\kappa = 1/\sqrt{2}$.

IV. VORTEX LATTICES

The energy of an ensemble of vortices is a nonlinear function of the vortex positions. It can be reduced to the pairwise vortex interaction (8) only in the case of large vortex separation. Then, in the nearest-neighbor approximation, the energy of the regular lattice of one-quantum vortices with lattice constant $l \gg 1$, calculated with respect to the uniform Meissner state, can be written as

$$f_{\text{lat}} = \frac{\bar{b}}{2\pi} \varepsilon_1 + \frac{\bar{b}}{2\pi} \frac{z}{2} U_{\text{int}}(l), \qquad (19)$$

where ε_1 is the one-vortex energy, z is the coordination number, and $\bar{b}/2\pi$ is the vortex density. The average magnetization $\bar{b}$ of the lattice is related to the unit cell area S_l of the vortex lattice:

$$\bar{b} = 2\pi/S_l. \qquad (20)$$

For equilateral triangular (with $z = 6$) and square (with $z = 4$) lattices it is $\bar{b}_\square = 2\pi/l^2$ and $\bar{b}_\triangle = 4\pi/l^2\sqrt{3}$.
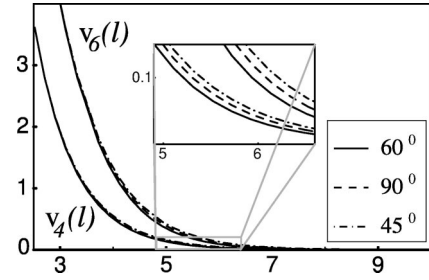
At closer distance between vortices the energy f_{lat} is renormalized both because of the next-nearest-neighbor vortex interaction and because of the nonlinear corrections. The first contribution can be accounted for by a redefinition of $U_{\text{int}}(l)$ as $U_{\text{int}}(l) + U_{\text{int}}(\sqrt{3}l)$ for a triangular and $U_{\text{int}}(l) + U_{\text{int}}(\sqrt{2}l)$ for a square lattice.

However, the nonlinear corrections can only be calculated by a vortex-lattice solution of the BJR equation (3). In fact one can extend Eq. (19) to the case of arbitrary l provided that the contribution $(z/2)U_{\text{int}}(l)$ is substituted with the interaction energy $(z/2)U_{\text{lat}}(l)$ calculated from the numerical solution of the BJR equation for a periodic vortex lattice. Similar to the case of two vortices, the energy can be expressed as

$$\frac{z}{2} U_{\text{lat}}(l) = (\gamma - c_4 t) v_4(l) - c_6 t v_6(l) \qquad (21)$$

via the lattice-dependent structure functions $v_k(l)$,

$$v_k(l) = \int [1 - |\psi_l(\mathbf{r})|^k] dS_l - \int [1 - |\psi_\infty(\mathbf{r})|^k] dS_\infty. \qquad (22)$$

The vortex lattice order parameter $|\psi_l(\mathbf{r})|$ is obtained from a numerical solution of Eq. (3), applying the method discussed in Sec. II to a unit cell S_l with periodic boundary conditions. The one-vortex solution $|\psi_\infty(\mathbf{r})|$ is calculated on an infinite unit cell S_∞. In Fig. 4 we show as an example the structure functions $v_k(l)$ for the triangular, square, and rhombic lattices.

The vortex interaction $(z/2)U_{\text{lat}}(l)$ depends on the control parameter d. Here we limit our discussion to the most realistic case $c_4 > 0, c_6 < 0$. We find a nonmonotonous behavior at $d < d_{c1} = 3$ with long-range attraction, short-range repulsion, and a minimum at intermediate distances as shown in Fig. 5 (thus we deal with the usual type-II superconductor case when $d > 3$ and the type-I superconductor when $d < 1$). We have considered all the simple lattices of the form shown in Fig. 6 and, in a nonsystematic way, some other lattices (multiquantum and four-cluster lattices). Among these, the lowest energy has always been found for a triangular lattice.
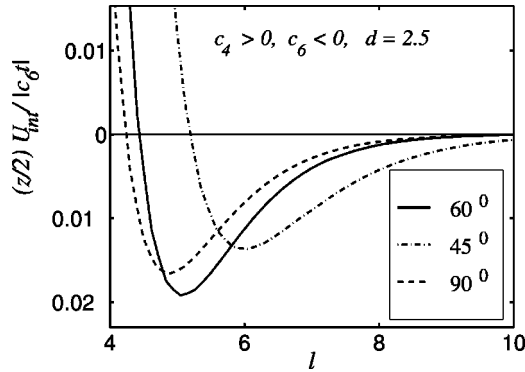
FIG. 5. The reduced vortex interaction energy $[zU_{lat}(l)]/(2|c_6 t|)$ in square (90°), triangular (60°), and rhombic (45°) lattices at $d=2.5$.

The most important consequence of the nonmonotonous vortex interaction is the existence of a special class of superconductors that are intermediate between type I and type II (we call them type I/II). They are characterized by a discontinuity of the transition between the Meissner and vortex states. A survey of properties of these superconductors has been given in our previous publication,[11] where we have demonstrated their existence in the interval $1<d<3$. We discuss now the details of the Meissner-vortex transition in type-I/II superconductors based on the the expression (21) calculated above.

The stability of the vortex lattice in an external magnetic field h_0 can be investigated by minimizing

$$f(\bar{b})=f_{lat}(\bar{b})-f_s=\frac{\bar{b}}{2\pi}\left[\frac{z}{2}U_{lat}(l(\bar{b}))-2\pi(h_0-h_{c1})\right] \quad (23)$$

(f_s is the Meissner free energy) over $\bar{b}$ and different lattice types. As can be seen in Fig. 7 the transition from Meissner state with $\bar{b}=0$ to the vortex state with finite $\bar{b}$ in type-I/II superconductors occurs discontinuously at a critical field h_{c1}^* that is smaller than the field $h_{c1}=\varepsilon_1/2\pi$ where the penetration an individual vortex becomes energetically advantageous. The critical field h_{c1} which serves as the lower critical field of the continuous vortex–Meissner-state transition in type-II superconductors can be interpreted as the field of superheating for type-I/II superconductors.

Another important conclusion is that, among the different types of lattices studied here, the triangular one-quantum lat-
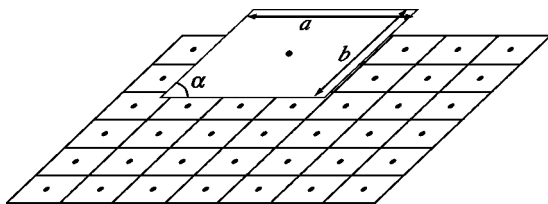
FIG. 6. Possible vortex lattice structures considered here, $1/6<a/b\leq 1, \pi/12\leq\alpha\leq\pi/2$.
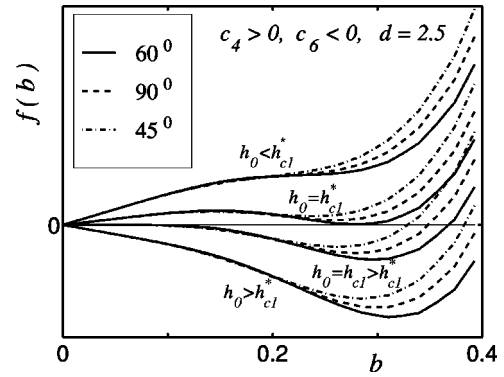
FIG. 7. Energy f of the different vortex lattices as a function of $\bar{b}$ in an external field h_0. The minimum of $f(\bar{b})$ corresponds to the most stable vortex state at a given h_0. The Meissner state corresponds to $\bar{b}=0$. The lattice constant l is inversely proportional to $\bar{b}^{1/2}$. The material parameter d is the same as in Fig. 5.

tice is the most stable one. We can show this numerically for all values of d and h_0 except for the interval $2.7<d<3, h_0 \sim h_{c1}^*$, where due to the large distance between vortices the accuracy of our calculation has been insufficient to draw definitive conclusions.

In Fig. 8 we show the magnetization jump $4\pi\Delta m =\bar{b}(h_{c1}^*)$ at the h_{c1}^* transition as a function of d. Flux expulsion varies from almost complete as in type-I superconductors at $d=1$ to vanishingly small at $d=3$ as in type-II superconductors. Surprisingly, we find that the jump Δm is almost linearly dependent on d between these two values. We also show the equilibrium lattice constant of the triangular lattice $l_\Delta=(\sqrt{3}\Delta z)^{-1/2}$ in Fig. 3 in order to compare it with the distance between vortices bound in a pair. At $d=1$ the distance between vortices in a lattice is minimal and equal to $l_\Delta=(4\pi/\sqrt{3})^{1/2}\approx 2.69$. The vortex distance in the lattice is larger than for the vortex pair, because the presence of other vortices suppresses superconductivity and thus diminishes the pressure of the superconducting phase against the vortices. At $d\to d_{c1}=3$ the vortex distance diverges and the lattice energy can be approximated as a superposition of pairwise interaction energies.

The discontinuity at the h_{c1}^* transition can be observed experimentally as a spinodal vortex clustering in the intermediate-mixed state in thin superconducting plates.[4] The properties of such clusters are determined by the delicate
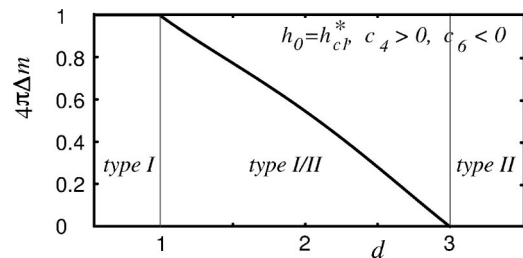
FIG. 8. Jump of magnetization $4\pi\Delta m=\bar{b}(h_{c1}^*)$ at the transition between vortex and Meissner state as function of the control parameter d (case $c_4>0, c_6<0$).

balance between the nonmonotonous vortex interaction $U_{lat}(l)$ and the vortex repulsion due to the additional interaction through the stray magnetic field energy in the vacuum outside the superconducting plate. Detailed calculations of this effect based on the explicit form of $U_{lat}(l)$ are currently in a progress.

*Permanent address: CSCS, Galleria 2, CH-6928 Manno, Switzerland. Electronic address: fawzi@cscs.ch

[1] L. Kramer, Phys. Rev. B **3**, 3821 (1971).

[2] L. Jacobs and C. Rebbi, Phys. Rev. B **19**, 4486 (1979).

[3] E.B. Bogomolnyi, Yad. Fiz. **24**, 861 (1976) [Sov. J. Nucl. Phys. **24**, 449 (1976)]; E.B. Bogomolnyi and A.I. Vainstein, *ibid.* **23**, 1111 (1976) [**23**, 588 (1976)].

[4] R. P. Hübener, *Magnetic Flux Structures in Superconductors* (Springer, Berlin, 1979), for a review of experiments.

[5] U. Krägeloh, Phys. Status Solidi **42**, 559 (1970).

[6] A.E. Jacobs, Phys. Rev. B **4**, 3022 (1971); see also **4**, 3029 (1971).

[7] G. Blatter and V. Geshkenbein, Phys. Rev. Lett. **77**, 4958 (1996).

[8] L. Neumann and L. Tewordt, Z. Phys. **189**, 55 (1966).

[9] A. Hubert, Phys. Status Solidi B **53**, 147 (1972).

[10] E.H. Brandt, Phys. Status Solidi B **77**, 105 (1976).

[11] I. Luk'yanchuk, Phys. Rev. B **63**, 174504 (2001).

[12] W. Bangerth, R. Hartmann, and G. Kanschat, deal. II *Differential Equations Analysis Library, Technical Reference*, IWR (2002), http://gaia.iwr.uni-heidelberg.de/~deal/.

[13] M. Ainsworth and A. Craig, Numer. Math. **60**, 429 (1991).

[14] W. Bangerth, in *Proceedings of the 16th IMACS World Congress 2000, Lausanne, Switzerland, 2000*, edited by M. Deville and R. Owens (2000), Document Sessions/118-1.